Photochemical OFF/ON Cytotoxicity Switching by Using a Photochromic Surfactant with Visible Light Irradiation

ACS OMEGA

http://pubs.acs.org/journal/acsodf

Article

Photochemical OFF/ON Cytotoxicity Switching by Using a Photochromic Surfactant with Visible Light Irradiation

Mai Shinohara, Yuya Ashikaga, Wei Xu, Sunnam Kim, Tuyoshi Fukaminato, Takuro Niidome, and Seiji Kurihara*

Cite This: *ACS Omega* 2022, 7, 6093−6098

Read Online

ACCESS | Metrics & More | Article Recommendations | Supporting Information

ABSTRACT: Photochemical switching of cytotoxicity by using spiropyran compounds with pyridinium and alkyl groups was investigated. The spiropyran compound, **SP6**, with a hexyl group as the alkyl group displayed negative photochromism, in which the hydrophilic open merocyanine form (MC form) was stable and isomerized to the hydrophobic closed spiro form (SP form) by visible light irradiation. Both MC and SP forms exhibited amphiphilicity because of the hydrophobic hexyl and hydrophilic pyridinium groups introduced. Cytotoxicity toward HeLa cells was observed for both MC and SP forms of **SP6** at concentrations higher than the critical aggregation concentration of the isomers CAC_{MC} and CAC_{SP} ($CAC_{MC} > CAC_{SP}$), respectively. In contrast, cytotoxicity by **SP6** was activated by visible light irradiation at concentrations between CAC_{MC} and CAC_{SP}; thus, photochemical switching of cytotoxicity from the OFF to ON state was achieved. Cytotoxicity was revealed to be caused by disruption of the cell membrane. The results provide an important step in developing novel next-generation photochemotherapy drugs.

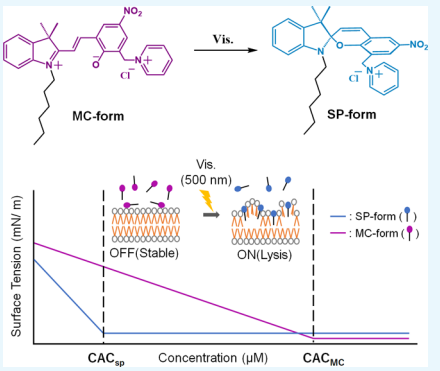

INTRODUCTION

Drugs can show side effects because of low specificity toward a target area. Control of the site of action, period of activity, and amount at the target site can improve the pharmacological effect of a drug while reducing side effects.[1−3] Light is a suitable external trigger for precise spatial control of drug activity because of factors such as coherency and external operation. Moreover, the light wavelength and intensity can be easily controlled. Since the pioneering work by Trauner, Thorn-Seshold, and co-workers in 2015,[4] the number of studies examining photochemical control of drug cytotoxicity by photochromic compounds has increased.[5−9]

In contrast to the use of photochromic compounds, Kobayashi et al. reported in 2011 near-infrared photoimmunotherapy (NIR-PIT), which is based on a photoactive molecule-conjugated antibody (mAb-IR700).[10,11] NIR-PIT treats cancer by irradiating cancer cells with NIR light after the conjugate binds to target cancer cells via an antigen−antibody reaction. Irradiation of cells with NIR light causes a change in hydrophobicity and shape of the conjugate, which ruptures cancer cells and induces necrotic cell death.[12−14] Importantly, NIR-PIT facilitates the release of tumor antigens by directly disrupting the stability of cell membranes, which subsequently activates the immune system against cancer cells. In NIR-PIT, antibodies used in the conjugates function by selective recognition of cancer cells as well as disruption of the cancer cells. Therefore, the reduced therapeutic efficiency of NIR-PIT may occur for cancer cells displaying only a few surface antigens.[15] In addition, the antibody can be expensive to prepare and must be modified to match the type of cancer targeted. Thus, modification of an antibody with photoactive molecules is a complex procedure that increases the cost of the therapeutic system. In this report, we constructed a light-responsive antigen release system where cell disruption is regulated by photochromic reaction without using antibodies (Figure 1).

We have focused on a surfactant, in particular a cationic surfactant, to develop a light-responsive antigen release system.

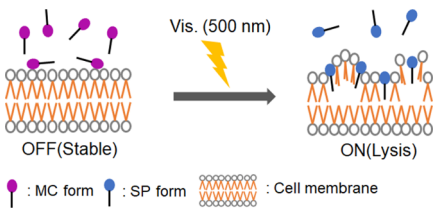

Figure 1. Schematic representation of cytolysis by **SP6** between CAC_{SP} and CAC_{MC}.

Received: November 17, 2021
Accepted: January 28, 2022
Published: February 11, 2022

https://doi.org/10.1021/acsomega.1c06473
ACS Omega 2022, 7, 6093−6098

Scheme 1. Photochromism of Spiropyrans

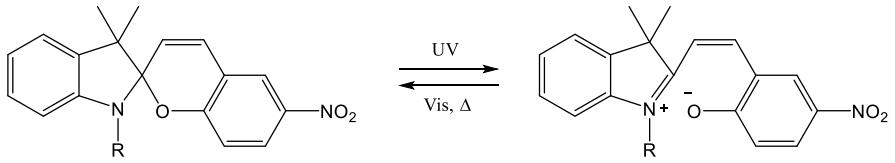

SP form (stable) MC form

Studies have reported the cytotoxicity of cationic surfactants toward cells[16,17] Moreover, the cytotoxicity of cationic surfactants was reported to increase as the alkyl chain length of the cationic surfactants increased,[18] indicating that the cytotoxicity of the cationic surfactants increases as the hydrophobicity increases. The solubilization and disruption of the cell membrane integrity contribute to the cytotoxicity of cationic surfactants. Thus, controlling the hydrophobicity of cationic surfactants photochemically affords a candidate compound where cell disruption can be regulated. This concept prompted us to study photo-activating cytotoxicity using a spiropyran compound with a cationic group.

Spiropyran compounds are standard photochromic compounds, in addition to azobenzene and diarylethene compounds that have been used for photo-activation of the aforementioned drugs.[19] Spiropyran compounds show photoisomerization between a closed spiro form (SP form) and an open merocyanine form (MC form) (Scheme 1). Photoisomerization provides a unique feature; the MC form is more hydrophilic than the SP form because of the formation of zwitterion in the MC form. Here, it is noteworthy that the ratio of the SP form to MC form in the initial state is dependent on various conditions such as solvents and chemical structures, and interestingly, some spiropyrans with a hydrophilic group show a negative photochromism in which the colored hydrophilic MC form is stable in water and darkness and isomerizes photochemically to the colorless hydrophobic SP form. Therefore, alternating between the OFF and ON states of cell disruption activity should be possible by using such negative photochromic spiropyran compounds. In addition, the absorption wavelength of the colored MC form exists in the visible region. In most reports on photo-activating drugs, UV light is used for photo-activation.[5−9] UV light damages cells by chemically altering DNA and is easily scattered making penetration through tissue difficult. Therefore, a photochromic compound exhibiting sensitivity to visible light or near-infrared light is favored for applications in photochemical cancer therapy.

EXPERIMENTAL SECTION

Generals. General chemicals were purchased from Tokyo Chemical Industry, FUJIFILM Wako Pure Chemical Co., and Sigma-Aldrich Chemical Co. and used without further purification. ^{1}H NMR (400 MHz) spectra were recorded on a JEOL JNMEX400 spectrometer with tetramethylsilane (TMS) as the internal standard. Mass spectra were measured with a mass spectrometer (Autoflex Speed, Bruker). UV−Vis. absorption spectra were recorded on a Hitachi U-3310 spectrophotometer. Visible irradiation was carried out with a Lamp-type UV irradiation system (Hamamatsu, LIGHTNINGCURE, LC8) and a Cut-off filter (λ > 500 nm). The cell imaging was demonstrated using a fluorescence microscope (ZEISS) equipped with appropriate filters.

Syntheses. **SP1** and **SP12** were synthesized according to previous reports.[23−25] The synthesis of SP6 is described as follows.

3-Chloromethyl-5-nitrosalicylaldehyde (2). 5-nitrosalicylaldehyde (25.0 g, 150 mmol) and chloromethyl methyl ether (100 mL) were added in an ice bath (5 °C). $AlCl_3$ (16.0 g, 120 mmol) was added slowly, and then the solution was stirred for 24 h under an argon atmosphere. Water was added to the solution, and the resulting solid was recovered and purified by recrystallization from carbon tetrachloride. Yield: 29.0 g (90%, yellow solid). ^{1}H NMR (400 MHz, D2O): δ 4.70 (s, 2H), 8.53−8.56 (m, 2H), 10.01 (s, 1H), and 12.06 (s, 1H).

2-Hydroxy-3-formyl-5-nitrobenzylpyridinium Chloride (3). 3-Chloromethyl-5-nitrosalicylaldehyde 2 (0.53 g, 2.44 mmol) and pyridine (2.0 g, 25.2 mmol) were added to acetone (10 mL) and stirred for 6 h under an argon atmosphere. After evaporation, the precipitate was collected and washed with diethyl ether. Yield: 0.5 g (74%, yellow solid). ^{1}H NMR (400 MHz, D2O): δ 5.63 (s, 2H), 8.06 (t, J = 16 Hz, 2H), 8.33 (d, J = 4 Hz, 2H), 8.48 (d, J = 4 Hz, 1H), 8.7 (d, J = 8 Hz, 1H), 9.16 (d, J = 4 Hz, 2H), 10.08 (s, 1H).

1-Hexyl-2,3,3-trimethyl-3*H*-indol-1-ium Iodide (5). A solution of 2, 3, 3-trimethylindolenine (2.01 g, 12.6 mmol) and hexyl iodide (3.22 g, 15.2 mmol) was refluxed for 17 h under an argon atmosphere. After cooling to room temperature, the resulting solid was recovered and purified by precipitation with CH_2Cl_2/diethyl ether. Yield: 3.84 g (82%, black-purple solid). ^{1}H NMR (400 MHz, D2O): δ 0.83 (t, J = 16 Hz, 3H), 1.27−1.38 (m, 6H), 1.50 (s, 6H), 1.77−1.81 (m, 2H), 2.80 (s, 3H), 4.41 (t, J = 16 Hz, 2H), 7.59 (t, J = 8 Hz, 2H), 7.81 (t, J = 4 Hz, 1H), 7.93 (t, J = 12 Hz, 1H).

1-Hexyl-3′,3′-dimethyl-6-nitro-8-pyridiniomethyl-spiro-[2*H*-1-benzopyran-2,2′-indoline] Chloride (SP6). 40% NaOH aqueous solution (100 mL) was added to the iodide, the resulting mixture was stirred for 15 min. Then, the mixture was extracted with ether, and the organic layer was concentrated. The red-yellow oil that resulted was isolated (1.89 g, 7.7 mmol) and added to 2-hydroxy-3-formyl-5-nitrobenzylpyridinium chloride (3) (2.28 g, 7.7 mmol) in methanol (15 mL). The solution was reflexed for 24 h under an argon atmosphere. After evaporation of the solvent, the residue was purified by precipitation with CH_2Cl_2/hexane to give a black-purple solid (1.65 g, 41%). ^{1}H NMR (400 MHz, D2O): δ 0.62 (t, J = 16.0, 3H), 0.93−1.27 (m, 8H), 1.58 (s, 6H), 1.72−1.77 (m, 2H), 4.29 (t, J = 16.0 Hz, 2H), 5.52 (s, 2H), 7.45−7.56 (m, 4H), 7.73 (d, J = 16.0 Hz, 1H), 7.93 (t, J = 12 Hz, 2H), 8.23 (d, J = 16.0 Hz, 1H), 8.30 (s, 1H), 8.42 (t, J = 16.0 Hz, 1H), 8.48 (s, 1H), 8.83 (d, J = 4.0 Hz, 2H). Elemental analysis: calculated for $C_{30}H_{34}ClN_3O_3$ (+2.3H_2O) (%): C, 64.2; N, 7.5; H, 6.5. Found (%): C, 64.7; N, 7.5; H, 6.9.

Surface Tension Test to Obtain the CAC: Wilhelmy Plate Method. The CMC was obtained by measuring the

https://doi.org/10.1021/acsomega.1c06473
ACS Omega 2022, 7, 6093−6098

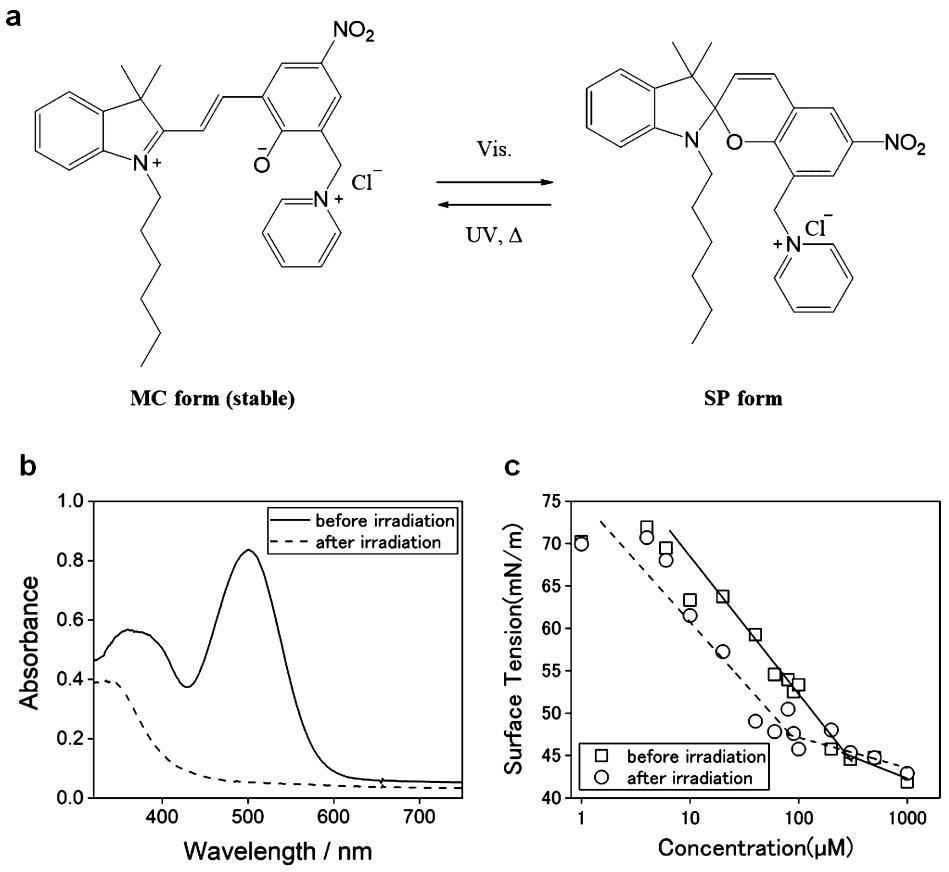

Figure 2. (a) Isomerization structures of negative photochromic spiropyran (**SP6**); open merocyanine form (MC form) and closed spiro form (SP form). (b) UV−vis absorption of **SP6** before (solid line) and after (broken line) visible light irradiation (λ > 500 nm, 8.0 mW/cm^2 for 15 min) in D-MEM with 10% FBS containing 10% water. (c) Surface tension measurements of **SP6** before (square) and after (circle) visible light irradiation (λ > 500 nm, 8.0 mW/cm^2 for 15 min) in water.

surface tension of SP1 and SP6 in deionized water at 37 °C, which were obtained using the Wilhelmy plate method. The Wilhelmy plate, which was a thin platinum plate, was cleaned thoroughly and attached to a force balance and then was brought into contact with a fluid. The force balance then measured the weight change caused by the contact of the plate with the meniscus using a tensiometer (KYOWA, DY-300).

Cell line and culture: HeLa cells were cultured in D-MEM (Wako Pure Chemical Industries, Japan) with 10% fetal bovine serum (FBS, Sigma-Aldrich, Japan) and 1% Antibiotic-Antimycotic Mixed Stock Solution (Nacalai Tesque, Japan) in a humidified atmosphere of 95% air and 5% CO_2 at 37 °C.

Cytotoxicity Assay. Cell Counting Kit-8 (CCK-8) assays of SP1 and SP6 with Hela cells were investigated. Cells were cultured on a 96-well cell-culture plate with a density of 1 × 10^5 cells per well. After culturing for 24 h, SP1 and SP6 at various concentrations (10, 50, 100, 200, 300, and 500 μM) dissolved in D-MEM with/without 10% FBS containing 10% water were added to the wells, and then visible light irradiation (λ > 500 nm, 8.0 mW/cm^2) was carried out for 15 min. Subsequently, the cells were incubated under 5% CO_2 at 37 °C for 15 min. After cleaning the wells with PBS to remove SP1 and SP6 residues, CCK-8 solution was added to each well and the cells were cultured for 3 h under the same conditions. Experiments without visible light irradiation were performed in the same procedure. When D-MEM with/without 10% FBS containing 10% water was the control, the absorbance (OD; optical density) of each well was measured at 490 nm with a microplate spectrophotometer system (WAKO, Infinite 50). The cell viability of SP1 and SP6 was calculated using the following formula

$$\text{Cell viability}(\%) = \frac{\text{OD}_{\text{treatment}}}{\text{OD}_{\text{control}}} \times 100\%$$

Cell Image. Cells were seeded in Glass Bottom Dishes and left to adhere for approximately 24 h before imaging experiments. SP6 stock solutions (50 and 100 μM) were prepared by dissolving in D-MEM with 10% FBS containing 10% water. The solutions were added to the dishes, and then visible light irradiation (λ > 500 nm, 8.0 mW/cm^2) was carried out for 15 min. Subsequently, the cells were incubated under 5% CO2 at 37 °C for 15 min. After cleaning the wells with PBS to remove SP6 residues, the cells were imaged at 40× magnification using a fluorescence microscope (ZEISS).

LDH Assay. Cytotoxicity LDH assay kit-WSTs of SP1 and SP6 with HeLa cells were investigated. The cells were cultured on a 96-well cell-culture plate with a density of 1 × 10^5 cells per well. After culturing for 24 h, SP1 and SP6 at various concentrations (10, 50, 100, 200, 300, 500, and 1000 μM) dissolved in D-MEM with 10% FBS containing 10% water were added to the wells and then visible light irradiation was carried out for 15 min (λ > 500 nm, 8.0 mW/cm^2). Subsequently, the cells were incubated under 5% CO_2 at 37 °C for 15 min. Lysis buffer was added to high control wells and incubated at 37 °C in a CO_2 incubator for 30 min. 100 μL of the working solution was added to each well and protected the

https://doi.org/10.1021/acsomega.1c06473
ACS Omega 2022, 7, 6093−6098

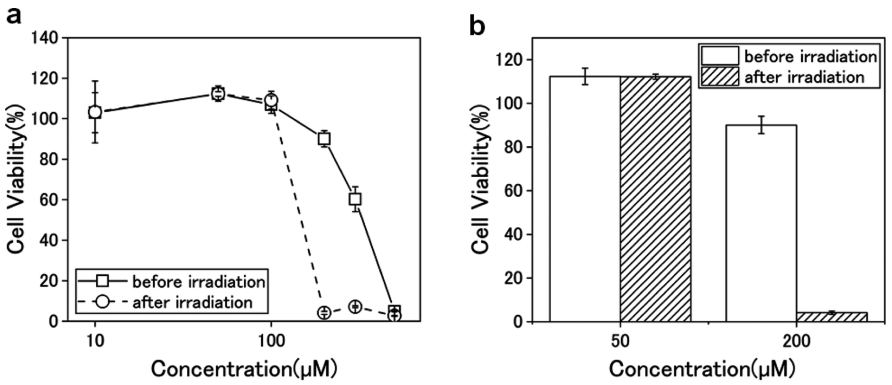

Figure 3. (a) HeLa cell viability determined by the CCK-8 assay for **SP6** before and after visible light irradiation (λ > 500 nm, 8.0 mW/cm^2 for 15 min) at different concentrations in D-MEM with 10% FBS containing 10% water. (b) Cell viability of **SP6** at 50 and 200 μM in D-MEM with 10% FBS containing 10% water before and after visible light irradiation (λ > 500 nm, 8.0 mW/cm^2 for 15 min).

plate from light and incubated at room temperature for 30 min. After that, 50 μL of stop solution was added to each well. Experiments without visible light irradiation were performed in the same procedure. When D-MEM with 10% FBS containing 10% water was the low control, the absorbance of each well was measured at 490 nm with a microplate spectrophotometer system (WAKO, Infinite 50). The LDH release of SP1 and SP6 was calculated using the following formula

$$\text{LDH release}(\%) = \frac{\text{OD}_{\text{treatment}} - \text{OD}_{\text{low control}}}{\text{OD}_{\text{high control}} - \text{OD}_{\text{low control}}} \times 100\%$$

RESULTS AND DISCUSSION

We explored the photochromic behavior of a water-soluble spiropyran compound with both hexyl and pyridinium groups in the molecule (**SP6**, Figure 2a) and its cytotoxicity with respect to change in hydrophobicity/hydrophilicity by the photochromic reaction. As shown in Figure 2b, the absorption band of **SP6** was observed at ~500 nm in D-MEM with 10% FBS containing 10% water and decreased noticeably upon visible light irradiation. The absorbance at 500 nm increased over time when light-irradiated **SP6** was placed in darkness (Figure S1). The results demonstrated that **SP6** exhibits negative photochromism with the stable colored hydrophilic MC form transforming into the colorless hydrophobic SP form by visible light irradiation (λ > 550 nm).[20,21] NMR analysis revealed that **SP6** molecules adopt predominantly (nearly 100%) the MC form in the equilibrium state in water and visible light irradiation caused photoisomerization to the SP form (Figure S2).

Spiropyrans with both pyridinium and long alkyl groups were reported to behave as surfactants.[22] Thus, to determine the surfactant properties of **SP6**, the surface tension of **SP6** in water was measured without/with visible light irradiation (λ > 550 nm) (Figure 2c). Typical surface tension−concentration profiles that indicated the formation of self-assemblies were obtained for SP and MC forms. The critical aggregation concentration (CAC) was found to differ between the SP and MC forms of **SP6**. The CAC of the SP form (CAC_{SP}) was lower when compared with that of the MC form (CAC_{MC}). The MC form is more hydrophilic when compared with the SP form because of the zwitterion of the MC form, which yields a higher CAC_{MC}. These results indicate that the self-assembly of **SP6** molecules in water can be controlled by visible light irradiation over the concentration range between CAC_{SP} and CAC_{MC}. Only a few self-assemblies of **SP6** at 100 μM were observed in water without visible light irradiation, whereas nonspherical assemblies of **SP6** were observed following visible light irradiation (Figure S3).

Next, cytotoxicity of **SP6** toward HeLa cells was examined by using the Cell Counting Kit-8 (CCK-8) assay. Figure 3a shows the dose−response curve between 10 and 500 μM **SP6** without/with visible light irradiation in D-MEM with 10% FBS containing 10% water. **SP6** is isomerized to the SP form with visible light irradiation, but in this cell viability experiment, it is estimated that 9% of them thermally recovered to the MC form, considering the incubation time after light irradiation, and the result of the thermal recovery experiment is shown in Figure S1. Although not in 100% SP form, most **SP6** above 90% existed in the SP form. Therefore, it is demonstrated that **SP6** exhibited clear dose-dependent cytotoxicity, and cytotoxicity of the SP form was higher when compared with that of the MC form. As shown in Figures 3b and S4 (microscopic images of HeLa cell), there was no difference in cell viability between the MC and SP forms of **SP6** at 50 μM. In contrast, a distinct difference was observed at 200 μM with cell viabilities of 90 and 4% observed without and with visible light irradiation, respectively. Thus, significant activation in cytotoxicity was achieved by photoisomerization from the hydrophilic MC form to the hydrophobic SP form.

The lactate dehydrogenase (LDH) release assay was used to determine the cytotoxic mechanism of **SP6**. Figure 4 shows the changes in LDH release from HeLa cells as a function of **SP6**

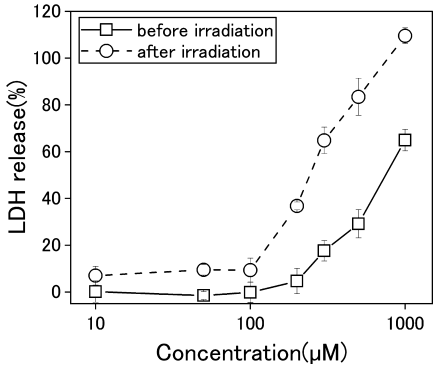

Figure 4. Change in LDH release as the **SP6** concentration increased in D-MEM with 10% FBS containing 10% water before and after visible light irradiation (λ > 500 nm, 8.0 mW/cm^2 for 15 min).

https://doi.org/10.1021/acsomega.1c06473
ACS Omega 2022, 7, 6093−6098

concentration without/with visible light irradiation. LDH release was found to increase at concentrations greater than ~200 μM, with LDH release clearly stronger for cells exposed to the SP form than for the MC form. The concentration dependence of LDH release is similar to the observed cytotoxicity. The results suggest that damage to the cell membrane of HeLa cells is induced by **SP6** molecules interacting with the cell membrane at higher concentrations. In particular, **SP6** molecules in the SP form caused efficient membrane damage, leading to higher cytotoxicity. Comparison of the concentration dependency of **SP6** cytotoxicity with LDH release and surface tension results indicated that the higher cytotoxicity of the SP form when compared with that of the MC form is related to the lower CAC_{SP}. A distinct increase in cytotoxicity was observed for MC and SP forms at concentrations near or higher than the CAC_{MC} and CAC_{SP}, respectively. At higher concentrations than the CAC, surfactant molecules cluster together to form assemblies in water. In an aqueous solution, the bilayer of the cells is less hydrophilic than the aqueous phase around the cells. **SP6** molecules, whether in the MC form or the SP form, not only form self-assemblies but also distribute in the cellular membrane above the CAC. The assembled structures are reversible between aggregation and dissolution. The aggregates are involved in surfactant activities that induce a fusion of surfactant molecules to the cell membrane and/or a solubilization effect.[17,26] As a result, both MC and SP forms disrupted the membrane above the CAC, leading to cell death.

The CAC is dependent on biological conditions, as the concentration of cytotoxicity changed in D-MEM with and without FBS, as shown in Figures 3a and S5. However, CAC can be used as an indicator to compare the properties of surfactants between the MC form and SP form. The SP form is still more hydrophobic than the MC form in cell buffer. This means that the SP form is more easily distributed to the cell membrane than the MC form. Therefore, the photochemical activation of cytotoxicity over the concentration range between the CACs of SP and MC forms can be explained as an increase in the amount of the **SP6** that translocates to the cell membrane because the hydrophobicity of the SP form is higher when compared with that of the MC form.

In contrast to **SP6**, **SP1** (Scheme S1) with a methyl group was found to exhibit a much lower cytotoxicity toward HeLa cells when compared with that of **SP6** because no change in cytotoxicity without/with visible light irradiation was observed. This lack of cytotoxicity is because of the higher hydrophilicity of **SP1** in both the MC and SP forms (Figure S6), which contrasts the water-insoluble **SP12** (Scheme S1) with a dodecyl group. Minor changes in both surface tension and LDH release were observed for various concentrations of **SP1**, and negligible activity was observed without/with visible light irradiation over the concentration range of 10−100 μM because of the higher hydrophilicity of **SP1** (Figure S6d). Thus, the balance of hydrophobicity and hydrophilicity of **SPn** molecules before/after photoisomerization is an important factor in developing compounds that show OFF/ON cell killing activity by damaging the cell membrane.

CONCLUSIONS

We have demonstrated that **SP6** with pyridinium and hexyl groups exhibits negative photochromism in which **SP6** molecules adopt predominantly the colored MC form in water. This MC form is isomerized to the SP form upon visible light irradiation, and the resulting SP form is more hydrophobic when compared with the MC form. Both the SP form and MC form were found to exhibit cytotoxicity (i.e., cell membrane damage) toward HeLa cells at concentrations higher than the CAC of the isomers. In addition, the photochemical change to **SP6** from the nontoxic to toxic form was achieved by visible light irradiation over the concentration range between CAC_{SP} and CAC_{MC}. This strategy is the first report of a photoactive surfactant drug that leads to the membrane disruption of cancer cells. Although some limitations currently exist for applying **SP6** to cancer treatment such as concentration condition, efficiency, light wavelength, and so on, there is no doubt that it plays an important role as a new concept. We continue to research to design highly efficient switching molecules that do not require special concentration conditions so that this strategy can be applied as a trigger for developing novel next-generation photochemotherapy and photoimmunotherapy drugs.

ASSOCIATED CONTENT

Supporting Information

The Supporting Information is available free of charge at https://pubs.acs.org/doi/10.1021/acsomega.1c06473.

Synthetic scheme and ^{1}H NMR spectra of SP6, TEM image of aggregates, microscopy image of cells, HeLa cell viability of SP6 without FBS, experimental results for SP1, UV−Vis absorption spectra, surface tension, cell viability, and LDH release (PDF)

AUTHOR INFORMATION

Corresponding Author

Seiji Kurihara − *Department of Applied Chemistry & Biochemistry, Graduate School of Science & Technology, Kumamoto University, Kumamoto 860-8555, Japan*; Email: kurihara@gpo.kumamoto-u.ac.jp

Authors

Mai Shinohara − *Department of Applied Chemistry & Biochemistry, Graduate School of Science & Technology, Kumamoto University, Kumamoto 860-8555, Japan*

Yuya Ashikaga − *Department of Applied Chemistry & Biochemistry, Graduate School of Science & Technology, Kumamoto University, Kumamoto 860-8555, Japan*

Wei Xu − *Department of Applied Chemistry & Biochemistry, Graduate School of Science & Technology, Kumamoto University, Kumamoto 860-8555, Japan*

Sunnam Kim − *Department of Applied Chemistry & Biochemistry, Graduate School of Science & Technology, Kumamoto University, Kumamoto 860-8555, Japan*; orcid.org/0000-0001-5039-7569

Tuyoshi Fukaminato − *Department of Applied Chemistry & Biochemistry, Graduate School of Science & Technology, Kumamoto University, Kumamoto 860-8555, Japan*; orcid.org/0000-0001-5504-0964

Takuro Niidome − *Department of Applied Chemistry & Biochemistry, Graduate School of Science & Technology, Kumamoto University, Kumamoto 860-8555, Japan*; orcid.org/0000-0002-8070-8708

Complete contact information is available at: https://pubs.acs.org/10.1021/acsomega.1c06473

https://doi.org/10.1021/acsomega.1c06473
ACS Omega 2022, 7, 6093−6098

Notes

The authors declare no competing financial interest.

■ ACKNOWLEDGMENTS

This research was funded by Japan Science and Technology Agency (JST), Core Research for Evolutional Science and Technology (CREST) (Grant Number JPMJCR18H5) and JP16H06506 in Scientific Research on Innovative Areas "Nano-Material Optical-Manipulation. We thank Edanz Group (https://en-author-services.edanzgroup.com/ac) for editing a draft of this manuscript.

■ REFERENCES

(1) Velema, W. A.; Szymanski, W.; Feringa, B. L. Photopharmacology: Beyond Proof of Principle. *J. Am. Chem. Soc.* **2014**, *136*, 2178−2191.
(2) Hüll, K.; Morstein, J.; Trauner, D. In Vivo Photopharmacology. *Chem. Rev.* **2018**, *118*, 10710−10747.
(3) Pianowski, Z. L. Recent Implementations of Molecular Photoswitches into Smart Materials and Biological Systems. *Chem. Eur. J.* **2019**, *25*, 5128−5144.
(4) Borowiak, M.; Nahaboo, W.; Reynders, M.; Nekolla, K.; Jalinot, P.; Hasserodt, J.; Rehberg, M.; Delattre, M.; Zahler, S.; Vollmar, A.; Trauner, D.; Thorn-Seshold, O. Photoswitchable Inhibitors of Microtubule Dynamics Optically Control Mitosis and Cell Death. *Cell* **2015**, *162*, 403−411.
(5) Engdahl, A. J.; Torres, E. A.; Lock, S. E.; Engdahl, T. B.; Mertz, P. S.; Streu, C. N. Synthesis, Characterization, and Bioactivity of the Photoisomerizable Tubulin Polymerization Inhibitor azo-Combretastatin A4. *Org. Lett.* **2015**, *17*, 4546−4549.
(6) Presa, A.; Brissos, R. F.; Caballero, A. B.; Borilovic, I.; Korrodi-Gregório, L.; Pérez-Tomás, R.; Roubeau, O.; Gamez, P. Photoswitching the Cytotoxic Properties of Platinum(II) Compounds. *Angew. Chem., Int. Ed.* **2015**, *54*, 4561−4565.
(7) Okuda, J.-y.; Tanaka, Y.; Kodama, R.; Sumaru, K.; Morishita, K.; Kanamori, T.; Yamazoe, S.; Hyodo, K.; Yamazaki, S.; Miyatake, T.; Yokojima, S.; Nakamura, S.; Uchida, K. Photoinduced cytotoxicity of a photochromic diarylethene via caspase cascade activation. *Chem. Commun.* **2015**, *51*, 10957−10960.
(8) Sheldon, J. E.; Dcona, M. M.; Lyons, C. E.; Hackett, J. C.; Hartman, M. C. T. Photoswitchable anticancer activity via trans-cis isomerization of a combretastatin A-4 analog. *Org. Biomol. Chem.* **2016**, *14*, 40−49.
(9) Cerón-Carrasco, J. P. Photooxidation of DNA as a key step in the cytotoxicity of photochromic diarylethenes. *Dyes Pigm.* **2017**, *142*, 530−534.
(10) Mitsunaga, M.; Ogawa, M.; Kosaka, N.; Rosenblum, L. T.; Choyke, P. L.; Kobayashi, H. Cancer cell-selective in vivo near infrared photoimmunotherapy targeting specific membrane molecules. *Nat. Med.* **2011**, *17*, 1685−1691.
(11) Kobayashi, H.; Choyke, P. L. Near-Infrared Photoimmunotherapy of Cancer. *Acc. Chem. Res.* **2019**, *52*, 2332−2339.
(12) Sato, K.; Ando, K.; Okuyama, S.; Moriguchi, S.; Ogura, T.; Totoki, S.; Hanaoka, H.; Nagaya, T.; Kokawa, R.; Takakura, H.; Nishimura, M.; Hasegawa, Y.; Choyke, P. L.; Ogawa, M.; Kobayashi, H. Photoinduced Ligand Release from a Silicon Phthalocyanine Dye Conjugated with Monoclonal Antibodies: A Mechanism of Cancer Cell Cytotoxicity after Near-Infrared Photoimmunotherapy. *ACS Cent. Sci.* **2018**, *4*, 1559−1569.
(13) Ogawa, M.; Tomita, Y.; Nakamura, Y.; Lee, M.-J.; Lee, S.; Tomita, S.; Nagaya, T.; Sato, K.; Yamauchi, T.; Iwai, H.; Kumar, A.; Haystead, T.; Shroff, H.; Choyke, P. L.; Trepel, J. B.; Kobayashi, H. Immunogenic cancer cell death selectively induced by near infrared photoimmunotherapy initiates host tumor immunity. *Oncotarget* **2017**, *8*, 10425−10436.
(14) Nagaya, T.; Friedman, J.; Maruoka, Y.; Ogata, F.; Okuyama, S.; Clavijo, P. E.; Choyke, P. L.; Allen, C.; Kobayashi, H. Host Immunity Following Near-Infrared Photoimmunotherapy Is Enhanced with PD-1 Checkpoint Blockade to Eradicate Established Antigenic Tumors. *Cancer Immunol. Res.* **2019**, *7*, 401−413.
(15) Sidransky, D. Emerging molecular markers of cancer. *Nat. Rev. Cancer* **2002**, *2*, 210−219.
(16) kaur, G.; Garg, P.; Kaur, B.; Chaudhary, G. R.; Kumar, S.; Dilbaghi, N.; Hassan, P. A.; Aswal, V. K. Synthesis, thermal and surface activity of cationic single chain metal hybrid surfactants and their interaction with microbes and proteins. *Soft Matter* **2019**, *15*, 2348−2358.
(17) Lichtenberg, D.; Ahyayauch, H.; Goñi, F. M. The Mechanism of Detergent Solubilization of Lipid Bilayers. *Biophys. J.* **2013**, *105*, 289−299.
(18) Wu, S.; Zeng, L.; Wang, C.; Yang, Y.; Zhou, W.; Li, F.; Tan, Z. Assessment of the cytotoxicity of ionic liquids on Spodoptera frugiperda 9 (Sf-9) cell lines via in vitro assays. *J. Hazard. Mater.* **2018**, *348*, 1−9.
(19) Szymański, W.; Beierle, J. M.; Kistemaker, H. A.; Velema, W. A.; Feringa, B. L. Reversible Photocontrol of Biological Systems by the Incorporation of Molecular Photoswitches. *Chem. Rev.* **2013**, *113*, 6114−6178.
(20) Kawanishi, Y.; Seki, K.; Tamaki, T.; Sakuragi, M.; Suzuki, Y. Tuning reverse ring closure in the photochromic and thermochromic transformation of 1′,3′,3′-trimethyl-6-nitrospiro[2H-1-benzopyran-2,2′-indoline] analogues by ionic moieties. *J. Photochem. Photobiol., A* **1997**, *109*, 237−242.
(21) Narachevsky, V. A. Negative photochromism in organic systems. *Rev. J. Chem.* **2017**, *7*, 334−371.
(22) Tazuke, S.; Kurihara, S.; Yamaguchi, H.; Ikeda, T. Photochemically triggered physical amplification of photoresponsiveness. *J. Phys. Chem.* **1987**, *91*, 249−251.
(23) Taylor, L. D.; Davis, R. B. The Chloromethylation of 5-Nitrosalicylaldehyde. *J. Org. Chem.* **1963**, *28*, 1713.
(24) Aldoshin, S. M.; Sanina, N. A.; Minkin, V. I.; Voloshin, N. A.; Ikorskii, V. N.; Ovcharenko, V. I.; Smirnov, V. A.; Nagaeva, N. K. Molecular photochromic ferromagnetic based on the layered polymeric tris-oxalate of Cr(III), Mn(II) and 1-[(1′,3′,3′-trimethyl-6-nitrospiro[2H-1-benzopyran-2,2′-indoline]-8-yl)methyl]pyridinium. *J. Mol. Struct.* **2007**, *826*, 69−74.
(25) Roxburgh, C. J.; Sammes, P. G.; Abdullah, A. Steric and substituent control on the photoreversibility of some novel N-alkyl-3,3′-disubstituted-6-nitro-indolospirobenzopyrans: Evaluation using UV spectroscopic studies. *Dyes Pigm.* **2011**, *90*, 146−162.
(26) Wang, D.; Richter, C.; Rühling, A.; Hüwel, S.; Glorius, F.; Galla, H.-J. Anti-tumor activity and cytotoxicity in vitro of novel 4,5-dialkylimidazolium surfactants. *Biochem. Biophys. Res. Commun.* **2015**, *467*, 1033−1038.

https://doi.org/10.1021/acsomega.1c06473
ACS Omega 2022, 7, 6093−6098